

Article

Quantum Heat Machines Equivalence, Work Extraction beyond Markovianity, and Strong Coupling via Heat Exchangers

Raam Uzdin ^{*}, Amikam Levy and Ronnie Kosloff

Fritz Haber Research Center for Molecular Dynamics, Hebrew University of Jerusalem, Jerusalem 9190401, Israel; amikamlevy@gmail.com (A.L.); kosloff1948@gmail.com (R.K.)

^{*} Correspondence: raam@mail.huji.ac.il

Academic Editor: Jay Lawrence

Received: 3 March 2016; Accepted: 31 March 2016; Published: 6 April 2016

Abstract: Various engine types are thermodynamically equivalent in the quantum limit of small “engine action”. Our previous derivation of the equivalence is restricted to Markovian heat baths and to implicit classical work repository (e.g., laser light in the semi-classical approximation). In this paper, all the components, baths, batteries, and engines, are explicitly taken into account. To neatly treat non-Markovian dynamics, we use mediating particles that function as a heat exchanger. We find that, on top of the previously observed equivalence, there is a higher degree of equivalence that cannot be achieved in the Markovian regime. Next, we focus on the quality of the battery charging process. A condition for positive energy increase and zero entropy increase (work) is given. Moreover, it is shown that, in the strong coupling regime, it is possible to super-charge a battery. With super-charging, the energy of the battery is increased while its entropy is being reduced at the same time.

Keywords: quantum heat engines; quantum refrigerators; quantum thermodynamics; heat exchanger; engine equivalence; two-stroke; four-stroke; non-Markovian; strong coupling

1. Introduction

All heat engines, classical and quantum, extract work from heat flows between at least two heat baths. When the working fluid is very small and quantum, e.g., just a single particle, the dynamics of the engine can be very different from that of classical engines [1,2]. Nonetheless, some classical thermodynamic restrictions are still valid. For example, quantum heat engines are limited by the Carnot efficiency even when the dynamics is quantum. Today, it is fairly well understood why the Clausius inequality originally conceived for steam engines still holds for small quantum heat machines.

The field of quantum thermodynamics has been intensively studied in recent years. The main research directions are the study of quantum heat machines, thermodynamic resource theory, and the emergence of thermal states. See the recent reviews [3–5] and references therein for more information on these research directions.

The study of quantum heat machines dates back to [6] where it was shown that the lasing condition for a system pumped by two heat baths corresponds to the transition from a refrigerator to an engine. See [7,8] for a more detailed analysis of such systems. Since then, various types of heat machines have been studied: reciprocating, continuous, autonomous and non autonomous, four-stroke machines, two-stroke machines, Otto engines and Carnot engines in the quantum regime. See [9–45] for a partial list on heat machine studies in recent years.

Experimentally, a single ion heat engine [46] and an NMR refrigerator [36] have already been built. Suggestions for realizations in several other quantum systems include quantum dots [47,48], superconducting devices [49–52], cold bosons [53], and optomechanical systems [34,54,55]. For other related experiments and their theoretical studies, see [56–60].

The second law was found to be valid for heat machines [9] in the weak system-bath coupling, where the Markovian dynamics is described by the Lindblad equation. In fact, the second law is consistent with quantum mechanics regardless of Markovianity as long as proper thermal baths are used [61]. One of the main challenges in this field is to find “quantum signatures” [1] in the operation of heat machines—more accurately, to find quantum signatures in *thermodynamic* quantities such as work, heat, and entropy production. Clearly, the engine itself is quantum and as such it may involve quantum features such as coherences and entanglement. The question is whether by measuring only thermodynamic quantities such as average heat or work, it is possible to distinguish between a quantum engine and a classical one.

As it turns out, there are thermodynamic effects that are purely quantum, the most relevant to this work is the equivalence of heat machine types [1]. Other quantum thermodynamic effects include extraction of work from coherences [62], oscillation in cooling [2], and multiparticle statistics effects [63]. In resource theory, it seems that quantum coherences in the energy basis also play an important role and impose restrictions on the possible single shot dynamics [64,65].

The traditional models and analysis of quantum heat machines resemble that of laser physics in the semi classical approximation. The driving field is often modeled by a classical electromagnetic field. This field generates a time-dependent Hamiltonian so it is possible to extract pure work from the system. When the classical field is replaced by a work repository (battery) with quantum description, the dynamics become more complicated [66]. For example, for an harmonic oscillator battery, the initial state of the battery has to be fairly delocalized in energy to avoid entropy generation in the baths [30,67]. This is problematic since an oscillator always has a ground state. See [66] for a detailed account of this mechanism. In this work, we shall use multiple batteries to extract work by interacting with the engine via energy conserving unitary evolution. Interestingly, machines without classical fields have been previously studied [16,30,68]. However, the research goals in these studies are entirely different from those of the present study.

Another assumption that is almost always used in the analysis of heat machines is that of weak coupling to the bath. Weak coupling, initial product state assumption, and other approximations lead to the Lindblad equation for the description of the thermalization process. The Lindblad equation is widely used in open quantum systems and they describe very well the dynamics in many scenarios. In other scenarios, such as strong system-bath interactions, or for very short evolution times, the Lindblad equation fails [69]. In the scheme presented in this paper, we include heat exchangers. Their role is to enable non-Markovian engine dynamics while still using Markovian baths.

One of the goals of this paper is to show that heat machine equivalence goes beyond the classical field approximation, and also for very short times where the Markovian approximation does not hold.

A “stroke” of a quantum machine is defined in the following way [1]. It is an operation that takes place in a certain time segment. In addition, a stroke does not commute with the operations (strokes) that take place before or after it. This non commutativity is essential for thermodynamic machines. Without it, the system will reach a state that is compatible with all baths and batteries, and no energy flows will take place. Different machine types differ in the order of the non commuting operations. In a two-stroke machine, the first stroke generates simultaneous thermalization of two different parts of the machine (manifolds) to different temperatures. In the next stroke, a time dependent Hamiltonian couples the two manifolds and generates a unitary that reduces the energy of the system. The energy taken from the system is stored in a classical field or in a battery, and is referred to as work. In a four-stroke engine, the strokes are thermalization of the hot manifold, unitary evolution, thermalization of the cold manifold, and another unitary evolution. In the continuous machine, all terminals (baths and work repository) are connected simultaneously: hot bath, cold bath, and battery/classical field. In this paper, we shall refer to this machine as simultaneous and not continuous for reasons explained later on.

Due to the abovementioned non commutativity, different machines operate in a different manner, and, in general, their performances differ (even in cases where they have the same efficiency as in the

numerical examples in [1]). Nonetheless, the thermodynamic equivalence principle presented in [1] states that in the quantum limit of small action, all machine types are thermodynamically equivalent. That is, they have the same work per cycle, and the same heat flows per cycle. This equivalence takes place where the operation of each stroke is very close to the identity operation. This regime is characterized by “engine action” that is small compared to \hbar . This does not mean low power since a small action cycle can be completed in a short time. Regardless of how close to identity the operations are, the different machine types exhibit very different dynamics (for example, the simultaneous machine does not have a pure unitary stage). Nevertheless, the equivalence principle states that all these differences disappear when looking at the *total heat or total work after an integer number of cycles*. The details of the equivalence principle will become clear as we present our results for the non-Markovian case.

The paper is organized as follows. Section 2 describes the engine and baths setup and introduces the heat exchangers. In Section 3.1, we derive the equivalence relation in the non-Markovian regime (short evolution time or strong couplings). The equivalence of heat machine types is valid when the “engine action” is small compared to \hbar . In Section 3.2, it is shown how to choose the initial state of the batteries in the weak action regime so that their entropy will not change in the charging process is shown. In addition, we find that, for large action, a different initial battery state is preferable. In the end of the section, it is shown that, for some initial states of the battery, the machine charges the battery with energy while reducing the entropy of the battery at the same time (super-charging). Section 3.3 shows that, in contrast to Markovian machines, it is possible to construct machines with a higher degree of equivalence. The emphasis is on the very existence of such machines, because their usefulness is presently unclear. In Section 4, we conclude the paper.

2. The Setup

We describe here the minimal model needed for extending the equivalence principle to short time dynamics beyond the Markovian approximation. However, the same logic and tools can be applied to more complicated systems with more levels or more baths. The setup studied in this paper is shown in Figure 1. Heat is transferred from the bath to the engine (black ellipse) via particles of the heat exchangers (circles on gears). In each engine cycle, the gears turn and a fresh particle enters the interaction zone (gray shaded area) where it stays until the next cycle. The engine can only interact with the particles in the interaction zone. The work repository is a stream of particles, or batteries, (green circles) that are “charged” with work by the engine. This interaction of the elements with the engine can be turned on and off as described by the periodic functions $f_k(t) = f_k(t + \tau_{cyc})$, where τ_{cyc} is the machine cycle time. Throughout the paper, we shall use the index “k” as a “terminal index” that can take the values “h”, “c” or “w” that stand for hot, cold and work repository (battery), respectively. In what follows, we elaborate on the different elements in the scheme.

2.1. The Heat Exchanger and the Baths

The heat machine equivalence principle [1] calls for a small engine action, which reads in the present formalism $\|H_{ek}\| \tau \ll \hbar$. However, in the microscopic derivation of the Lindblad equation, a rotating wave approximation is made. The approximation is valid only if τ is large compared to the oscillation time. This implies that $\|H_{ek}\|$ has to be very small in the equivalence regime. Nevertheless, in principle, small action can be achieved with strong (or weak) coupling $\|H_{ek}\|$ and short evolution time as long as $\|H_{ek}\| \tau \ll \hbar$ holds. In this regime, which is the subject of this paper, the dynamics is highly non-Markovian. Non-Markovian bath dynamics is, in general, very complicated and strongly depend on the specific bath realization. Heat machines and the second law in the presence of strong coupling have been discussed in [70–72].

To overcome the complicated dynamics and *to obtain results that are universal and not bath-realization dependent, we add heat exchangers to our setup*. Heat exchangers are abundant in macroscopic heat machines. In house air conditioning, a coolant fluid is used to pump heat from the interior space to an

external cooling unit. Water in a closed system is used in car engines to transfer heat to the radiator where air can cool the water. Perhaps the simplest example is the cooling fins that are used to cool devices like computer chips. The metal strongly interacts with the chip and conduct the heat to the fins. Then, the weak coupling with the air cools the fins. The interaction with the air is weak but, due to the large surface, it accumulates into a large heat transfer that cools the chip.

In the quantum regime, heat exchangers enable the following simplifications. Firstly, they separate the system interaction scales from the bath interaction scales. The system can undergo non-Markovian dynamics with the heat exchangers while the baths can thermalize the heat exchangers using standard weak coupling Markovian dynamics. Secondly, they enable starting each engine cycle with a known environment state (the particles in the interaction zone). Most importantly, this environment state is in a product state with the system and contains no memory of previous cycles. Thirdly, it eliminates the dependence on all bath parameters except the temperature. This means that, from the point of view of the machine, all different bath realizations are equivalent. This bath parameter independence holds as long as the bath fully thermalizes the heat exchanger particles.

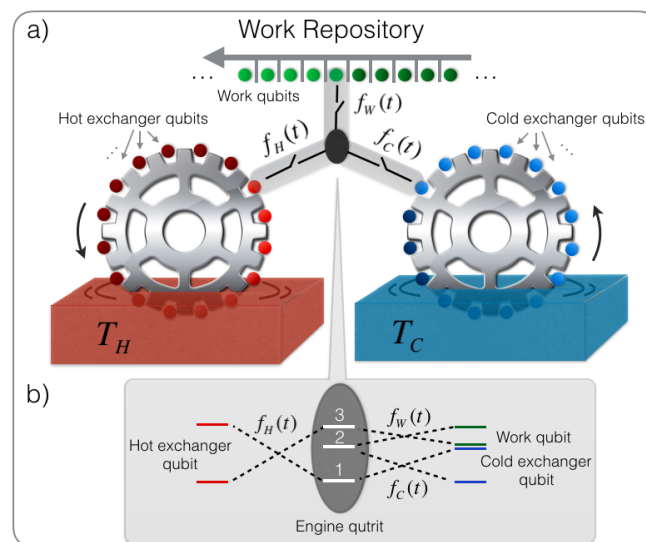


Figure 1. (a) heat machine scheme with heat exchangers (gears). Various engine types can be implemented in this scheme by controlling the coupling function $f_{c,h,w}(t)$ to the engine (ellipse). In each cycle, the gears turn and the work repository shifts so that new particles enter the interaction zone (gray shaded area). The heat exchangers enable the use of Markovian baths while having non-Markovian engine dynamics. This includes strong coupling and/or short time evolution. In this model, the work is stored in many batteries (work qubit in green); (b) the engine level diagram. This machine is based on two-body energy conserving unitaries. This is in contrast to other machines that employ three-body interaction.

In our scheme, the coolant fluids consist of N_c and N_h particles in each heat exchanger (particles around the gears in Figure 1a). The particles in the gear cyclically pass through the bath and the machine interaction zone (gray shaded area) with periods of $N_{c,h}\tau_{cyc}$. Note that the gears in Figure 1a are merely an illustration of the heat exchanger concept. The heat exchanger can be realized, for example, by adjacent superconducting qubit or by moving neutral atoms with light. The particles may interact strongly and in a non-Markovian way with the system. On the other hand, the particles interact *weakly* with the bath but for a sufficiently long time so that they fully thermalize when they leave the bath. After the exchanger particles exit the bath, they are in a thermal state and in a product state with the system (the bath removes all correlation to the machine). In each cycle of the engine, a different exchanger particle interacts with the system. $N_{c,h}$ are analogous to the size of the “cooling

fin". Their number is chosen so that within the Markovian, weak-coupling limit to the baths, for all practical purposes, they have sufficient time to fully thermalize.

Under the assumptions above, it does not matter what the exact details of the Markovian bath are (e.g., its thermalization time and correlation time). It only needs to induce thermal state via weak coupling (to avoid strong interaction issues). In this regime, the thermalization can be described by the Lindblad equation [69]. However, because of the heat exchanger full thermalization assumption, there is no need for an explicit solution.

The work repository is basically a heat exchanger without a bath. It may have a conveyor belt geometry as shown in Figure 1a, or it may be cyclic like the heat exchanger. The considerations of choosing the initial state of the batteries particles (work repository) will be discussed later.

The model can be extended by letting the system interact with more than one heat exchanger particle at a time, or by not fully thermalizing the particles. However, it seems like these types of extensions eliminate the advantages of using heat exchangers to begin with. The simple setup described above is sufficient to exemplify the equivalence principle in short time non-Markovian dynamics.

2.2. The Engine

The engine core shown in Figure 1b is a three-level system. Levels 1 and 3 constitute the hot manifold with an energy gap E_h , levels 1 and 2 constitute the cold manifold with a gap E_c , and the work manifold comprises levels 2 and 3. The more general notion of manifold separation in quantum heat machines is described in [1].

The hot (cold) manifold can interact only with the hot (cold) heat exchanger. This interaction can be switched on and off without any energetic cost as explained in the next section. The same holds for the work repository. If the engine qutrit interacts only with one heat exchanger, the hot for example, then the hot manifold of the system will eventually reach a Gibbs state at temperature T_h .

For the engine operating regime, we want the thermal strokes to create population inversion that would be used to excite the batteries to higher energies. This simple engine structure facilitates the construction of thermal machines using only two-body interactions rather than three-body interactions [16,30,68].

2.3. The Coupling of the Engine to the Heat Exchangers and to the Work Repository

In our model, the particles in the heat exchangers are all qubits. The energy gaps of the qubits in the heat exchangers are equal to the energy gaps of their corresponding manifold in the engine qutrit. As explained earlier, in each engine cycle, the heat exchanger dials turn and a new thermal particle is available to interact with the system. These exchanger particles are not initially correlated to the engine, so the initial state (in each cycle) of the particles in the engine interaction zone is $\rho_{tot}(t=0) = \rho_c \otimes \rho_h \otimes \rho_w \otimes \rho_e$ where ρ_e is the engine state and $\rho_{c,h,w}$ are the bath and work repository particles that are in the interaction zone of the system. The rest of the particles are not required until the next cycle of the machine.

The coupling between the engine and the hot bath particles has the form:

$$H_{int} = \sum_{k=c,h,w} f_k(t) H_{ek}, \quad (1)$$

where $f_k(t)$ are the controllable periodic scalar couplings (switches in Figure 1a and dashed lines in Figure 1b) introduced earlier. H_{ek} are energy conserving Hamiltonian: If H_k is the Hamiltonian of the exchanger particle and H_e is the qutrit engine Hamiltonian, then energy conserving interaction satisfies: $[H_{ek}, H_e + H_k] = 0$. This condition is the standard assumption in thermodynamic resource theory. It is used to define "thermal operations", and it ensures that energy is not exchanged with the controller that generates H_{ek} . The total energy in the exchangers, work repositories and the engine is not affected by H_{ek} . Thus, H_{ek} can only redistribute the total energy but not change it.

The simplest form of H_{int} is $H_{ek} = a_k a_{ek}^\dagger + a_k^\dagger a_{ek}$ where a_k is the annihilation operator for the k exchanger particle, and a_{ek} is the annihilation operator for hot manifold in the engine. These H_{ek} Hamiltonians generate a partial (or a full) swap between the k manifold in the machine and the terminal k . This operation is slightly more complicated than the standard partial swap as will be explained in the battery section.

In the beginning of each cycle, the engine starts in a product state with its immediate environment. This inserts a Markovianity scale to the model since there is no bath memory from cycle to cycle. Nonetheless, there are still important non-Markovian aspects in the intra-cycle dynamics. The full Markovian dynamics is obtained in the weak collision limit [73–77], where *in each thermal stroke*, the engine interacts weakly with *many particles of the heat exchanger*.

In the simultaneous machine, all the f_k are turned on and off together in order to couple the machine to different particles in the heat exchangers. Thus, the couplings are not fixed in time as in the Markovian continuous machine. While Markovian continuous machines do not have a cycle time, the simultaneous machines have a cycle time τ_{cyc} determined by the rate that particles of the heat exchangers enter the interaction zone.

2.4. The Work Repository

There are two major thermodynamic tasks: one is to produce work, and the other is to change the temperature of an object of interest. While cooling can be done either by investing work (power refrigerator) or by using only heat baths (absorption refrigerator), engines always involve the production of work. Often, the receiver of the work is not modeled explicitly. Instead, a classical field is used to drive the system and harvest the work. This is equivalent to a repository that is big and hardly changes its features due to the action of the engine.

When the work repository is modeled explicitly, various complications arise. First, the state of the battery may change significantly (especially if the battery starts close to its ground state) and therefore affect the operation of the engine (back action). Second, as entanglement starts to form between the battery and the system, the reduced state of the battery gains entropy. The energy exchange can no longer be considered as pure work. In an ideal battery, the energy increases without any accompanying entropy change. This feature is captured by the entropy pollution measure: $\Delta S / \Delta \langle E \rangle$ [78,79]. In a good battery, this number is very small and can even be negative as will be shown later.

To avoid the back action problem we will use multiple batteries. In the present scheme, it is sufficient to use qubits or qutrits. That is, instead of raising one weight by a large amount, we raise many weights just a little. In some cases, this is indeed the desired form of work. For example, an engine whose purpose is to prepare many particles with population inversion that are later used as a gain medium for a laser.

As with the heat exchanger, the batteries will be connected to the engine sequentially, one in each cycle (the $k = \omega'$ in Equation (1)). The reduced state of a terminal particle k (may belong to the heat exchanger or to the battery) after the engine operated on it, will be denoted by $\rho'_k = \text{tr}_{\neq j}[\rho'_{tot}]$. In general, after the cycle, the terminal particle may be strongly correlated to the engine.

The initial state of the battery is a key issue that dramatically affects the entropy pollution and the quality of charging the battery with work. Nevertheless, it is not directly related to the issue of heat machine equivalence so we will discuss the battery initial state only in Section 3.

2.5. Heat and Work

The heat that flows into the cold (hot) bath in one cycle is given by the change in the energy of the heat exchanger particle after one cycle:

$$Q_{c(h)}^{cycle} = \text{tr}[(U_{cyc} \rho_{tot}(0) U_{cyc}^\dagger - \rho_{tot}(0)) H_{c(h)} \otimes \mathbb{1}_{else}], \quad (2)$$

where U_{cyc} is the evolution operator generated by H_{int} over one cycle of the machine. Writing this in terms of the state of the whole system, rather than using the reduced state of the bath, is very useful. To evaluate the total change in the bath energy, we need to know the global transformation over one cycle U_{cyc} . The internal dynamics, which are machine dependent, have no impact on the total heat. All engines that have the same U_{cyc} will have the same amount of heat per cycle. This is in contrast to the equivalence in the Markovian Lindblad formalism [1]. There, a symmetric rearrangement theorem had to be applied to show that the total heat per cycle is the same for different machines. In the present case, when the one cycle evolution is equivalent for different types of machines, Equation (2) immediately implies equivalence of heat and work per cycle. Equivalence of all heat and work energy flows implies that the efficiency W/Q_h is the same as well for different machine types in the equivalence regime.

As for energy exchanges with the work repository $\Delta \langle H_w \rangle$, we replace $H_{c(h)}$ by H_w in Equation (2). In order to identify it with work, it is required that no entropy is generated in the work repository.

3. Results

3.1. The Equivalence of Heat Machines in the Non-Markovian Regime

The construction of various heat machine types in the same physical system was studied in [1], and it is based on operator splitting techniques. In particular, the Strang splitting [80–82] for two non commuting operators A and B is $e^{(A+B)dt} = e^{\frac{1}{2}Adt} e^{Bdt} e^{\frac{1}{2}Adt} + O(dt^3)$. Starting with the simultaneous machine operator where all terminals are connected simultaneously:

$$\begin{aligned} \tilde{U}_{cyc}^{simul} &= e^{-i[\mathcal{H}_e + \sum_{k=c,h,w} \mathcal{H}_k + \mathcal{H}_{ek}] \tau_{cyc}}, \\ &= U_0 U_{cyc}^{simul}, \end{aligned} \tag{3}$$

$$U_{cyc}^{simul} = e^{-i[\mathcal{H}_{ec} + \mathcal{H}_{eh} + \mathcal{H}_{ew}] \tau_{cyc}}, \tag{4}$$

where $U_0 = e^{-i(\mathcal{H}_e + \mathcal{H}_c + \mathcal{H}_h + \mathcal{H}_w) \tau_{cyc}}$, the single-particle coherence evolution operator can be singled out from the total evolution operator since $[\mathcal{H}_e + \mathcal{H}_c + \mathcal{H}_h + \mathcal{H}_w, H_{int}] = 0$. All of the population change is generated by U_{cyc}^{simul} . In fact, U_{cyc}^{simul} is the evolution operator in the interaction picture. Energy observables like heat look the same in the interaction picture ($U_0^\dagger H_{c,h,w} U_0 = H_{c,h,w}$). In practice, all states should be evolved with U_{cyc}^{simul} only. The bare Hamiltonians H_k are used only for calculating the energy observables. Thus, the single-particle coherences associated with interaction-free time evolution U_0 do not affect the population dynamics and observables like energy that are diagonal in the energy basis. The fact that U_0 commutes with U_{cyc}^{simul} means that outcome of the operation does not depend on the time the operation is carried out (time invariance).

This type of single-particle coherences should be distinguished from inter-particle coherences. Since the energy gaps in the machine and the terminal are matched, the inter-particle coherences are between degenerate states. For example, the states $|0_c 1_e\rangle$ and $|1_c 0_e\rangle$ are degenerate, and so are the pairs $\{|0_h 3_e\rangle, |1_h 0_e\rangle\}$ and $\{|0_w 3_e\rangle, |1_w 2_e\rangle\}$. The crossed lines in Figure 1b show the pairs of two-particle degenerate states. These inter-particle coherences are essential for the dynamics. Their complete suppression leads to a Zeno effect that halts all the dynamics in the engine. The inter-particle coherences are generated and modified by the interaction terms and hence cannot be separated from the rest of the evolution like the single-particle coherences. Note that changes in inter-particle coherence translate to population changes in the subspaces of individual particles.

When starting in a product state where the inter-particle coherences are zero, the energy transfer (population changes) is of order dt^2 while the coherence generation is of order dt . This is due to the fact that unitary transformation converts population to coherences and coherence to population (see Figure 8 in [1]). In thermodynamic resource theory, phases are often dismissed as non-essential, but we stress that this is true only for the single-particle coherences.

To study the relations between the simultaneous engine and the two-stroke engine, we apply the Strang decomposition which yields the following product form

$$\begin{aligned}
 U_{cyc}^{simul} &= e^{-i\mathcal{H}_{ew}\frac{\tau_{cyc}}{2}} e^{-i(\mathcal{H}_{ec}+\mathcal{H}_{eh})\tau_{cyc}} e^{-i\mathcal{H}_{ew}\frac{\tau_{cyc}}{2}} + O\left[\left(\frac{s}{\hbar}\right)^3\right], \\
 &= U^{II\ stroke} + O\left[\left(\frac{s}{\hbar}\right)^3\right],
 \end{aligned}
 \tag{5}$$

where s is the “engine norm action” $s = (\|\mathcal{H}_{ec}\|_{sp} + \|\mathcal{H}_{eh}\|_{sp} + \|\mathcal{H}_{ew}\|_{sp})\tau_{cyc}$ and $\|\cdot\|_{sp}$ is the spectral norm of the operator [1]. When this number is small compared to \hbar , $U_{cyc}^{II-stroke} \rightarrow U_{cyc}^{simul}$. Note that the first term and the third term in $U_{cyc}^{II-stroke}$ are two parts of the same stroke. The operator splits this way since the Strang splitting can only create symmetric units cells. A similar splitting can be done for the four-stroke engine exactly as shown in [1]. One immediate conclusion follows from the equivalence of the one cycle evolution operators: if different machine types *start in the same initial condition*, their state will coincide when monitored stroboscopically at $t_n = n\tau_{cyc}$. While at $t_n = n\tau_{cyc}$ the states of different machine types will differ by $O\left[\left(\frac{s}{\hbar}\right)^3\right]$ at the most, at other times they will differ by $O\left[\frac{s}{\hbar}\right]$. This expresses the fact that the machine types are never identical at all times. They differ in the strongest order possible $O\left[\frac{s}{\hbar}\right]$, unless complete cycles are considered. Since the one cycle evolution operators are equivalent, it follows from Equation (2) that *for the same initial engine state*:

$$Q_{h(c)}^{simul} \cong Q_{h(c)}^{II\ stroke} \cong Q_{h(c)}^{IV\ stroke}, \tag{6}$$

where Q^{simul} refers to the heat transferred in time of τ_{cyc} in the particle machine. The \cong stands for equality up to correction $\|H_{c(h)}\| O\left[\left(\frac{s}{\hbar}\right)^4\right]$. Note that the cubic term does not appear in Equation (6). Due to lack of initial coherence, the $O\left[\left(\frac{s}{\hbar}\right)^3\right]$ correction contributes only to the inter-particle coherence generation but not to population changes. Hence, the population changes differ only in order $O\left[\left(\frac{s}{\hbar}\right)^4\right]$. In transients, the system energy changes from cycle to cycle so, in general, it is not correct to use energy conservation to deduce work equality from heat equality. Nevertheless, work equality follows from Equations (2) and (5) when using H_w instead of $H_{c(h)}$.

This establishes the equivalence of heat (and work) even very far away from steady state operation or thermal equilibrium *provided all engines start with the same state*. This behavior is very similar to the Markovian equivalence principle [1], but there is one major difference. Since each cycle starts in a product state, the leading order in heat and work is $O\left[\left(\frac{s}{\hbar}\right)^2\right]$ and not $O\left[\frac{s}{\hbar}\right]$ as in the Markovian case. The linear term in the work originates from the single-particle coherence generated by the classical driving field. Without this coherence, the power scales as $(Q_h^{cyc} + Q_c^{cyc})/\tau_{cyc} \propto \tau_{cyc}$. Thus, as shown in Figure 2a, for small action, the power grows linearly with the cycle time. On the other hand, as explained earlier, the correction to the power is only of order $O\left[\left(\frac{s}{\hbar}\right)^4\right]/\tau_{cyc} = O\left[\left(\frac{s}{\hbar}\right)^3\right]$ since there is no cubic correction to the work.

Let us consider now the *steady state operation*. Despite Equation (6), it is not immediate that the heat will be the same for different machine types in steady state. In Equation (6), the initial density matrix is the same for all machine types. However, different types may have slightly different initial states, which may affect the total heat. To study equivalence in steady state operation, we first need to define what steady state means when the bath and batteries are included in the analysis. The whole system is in a continuous transient: the hot bath gets colder, the cold bath gets hotter, and the batteries are charged. Nonetheless, the reduced state of the engine relaxes to a limit cycle $\bar{\rho}_e(t) = \bar{\rho}_e(t + \tau)$ or explicitly $\bar{\rho}_e = tr_{\neq e}[U_{cyc}(\rho_c \otimes \rho_h \otimes \rho_w \otimes \bar{\rho}_e)U_{cyc}]$. To see the relation between steady states of different machines, we choose the steady state of one machine, for example $\bar{\rho}_e^{simul}$, and apply the two-stroke evolution operator to it:

$$\begin{aligned}
 \bar{\rho}'_e &= tr_{\neq e}[U_{cyc}^{II\ stroke}(\rho_c \otimes \rho_h \otimes \rho_w \otimes \bar{\rho}_e^{simul})U_{cyc}^{II\ stroke}] \\
 &= \bar{\rho}_e^{simul} + O\left[\left(\frac{s}{\hbar}\right)^4\right].
 \end{aligned}
 \tag{7}$$

The cubic order is absent because, if there are no initial inter-particle coherences, then the cubic term only generates inter-particle coherences. Hence, the reduced state of the system is not modified by the cubic correction of the two-stroke evolution operator. From Equation (7), we conclude that the steady states are equal for both machines up to quartic corrections in the engine action. From Equation (6), it follows that heat and work in steady state are also equal in all machine types, up to quartic correction. Figure 2a shows the power in steady state for the three main types of machines as well as for a higher order six-stroke machine that will be discussed in the last section. Let the power of the machine (work per cycle divided by cycle time) be denoted by P . In Figure 2b, we plot the normalized power P/P^{simul} where it is easier to see that the correction in the power of one machine with respect to the other is quadratic. This graph shows that the equivalence of non-Markovian machines is actually similar to that of Markovian machines. The difference is that the reference simultaneous power is constant (in action) in the Markovian case and linearly growing (small action) in the present case. Figure 2b shows that the equivalence is a phenomenon that takes place in a regime and not only at the (ill defined) point $\tau_{cyc} = 0$. The same holds for the Markovian case.

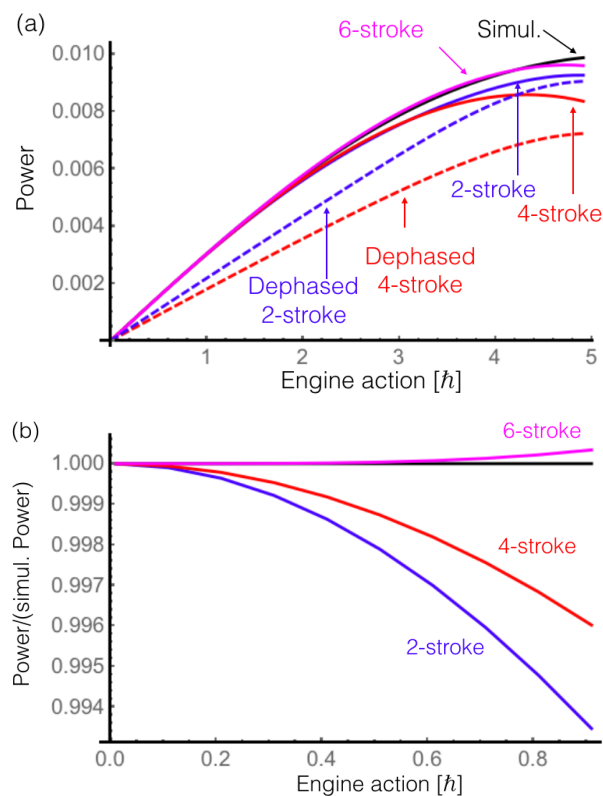


Figure 2. (a) In the non-Markovian regime the main machine types: four-stroke, two-stroke and simultaneous machine, have the same power when the engine action is small compared to \hbar . In contrast to the Markovian case here the power is not constant but grows linearly for small action. The action is increased by increasing the time duration of each stroke. The red and blue dashed curves show how the 4-stroke and 2-stroke engines are modified when a dephasing stroke is included. This demonstrates that the thermodynamic equivalence is a quantum coherence effect; (b) The equivalence become more visible when plotting the relative power of each machine with respect to the simultaneous machine. The 6-stroke machine, based on the Yoshida decomposition, is unique to the non-Markovian case and has a wider range of equivalence.

At this point, we wish to discuss the quantumness of the equivalence principle in the current setup. In [1], it was suggested to use dephasing in the energy basis to see if the machine is stochastic or quantum. If a dephasing stroke is carried out before the unitary stroke and the result is not affected,

then the machine operates as a stochastic machine. In the four-stroke engine and in the two-stroke engine described in Equation (5), the battery is accessed twice during the cycle. The first interaction with the battery creates some inter-particle coherence between the battery and the engine. As a result, the next interaction with the battery (the second work stroke) starts with nonzero inter-particle coherence. Thus, adding dephasing after the first work stroke will affect the power gained in the next work stroke. This is shown by the red and blue dashed curves in Figure 2a. The power of the simultaneous engine is zero if we continuously dephase the system (Zeno effect). We conclude that, although there is no coherence that carries over from one cycle to the next, as in the Markovian case, coherence is still needed for the equivalence principle to hold. This time, the coherence is an inter-particle coherence between degenerate states.

So far, we ignored the nature of the energy transferred to the battery, *i.e.*, if it is heat or work. If it is pure work, the device is an engine, whilst if it is heat, the device functions as an absorption machine (only heat bath terminals). However, the equivalence principle is indifferent to this distinction. If the action is small, two-stroke, four-stroke, and simultaneous machines will perform the same. In the next section, however, we study the conditions under which the entropy of the batteries is not increased and the device performs as a proper engine.

3.2. Work Extraction

3.2.1. The Initial State of the Battery in Strong and Weak Coupling

So far, we have not explicitly addressed the question of work extraction and whether the energy transferred to the batteries is actually pure work or heat. For engines, the goal is to make the entropy pollution $\Delta S_w / \Delta \langle H_w \rangle$ as small as possible. Figure 3 shows the well known expression for the entropy of a qubit as a function of the excited state population p_w . The von Neumann entropy and the Shannon entropy of single particles are identical since there are no single-particle coherences. The energy of the battery is proportional to the excited state population, so the x axis also indicates the energy of the battery. If the battery starts with a well defined energy state, that is the ground state $p_w = 0$, then a small increase in the energy will result in a large entropy generation in the battery. In fact, for small changes, this is the worst starting point (the origin in Figure 3). However, if we choose to start with a very hot battery at $p_w = 1/2$, ($T_w \rightarrow \infty$), the entropy increase will be very small if Δp_w is small. Thus, by using many batteries in a fully mixed state where each is only slightly changed ($\Delta p_w \ll 1$), it is possible to reach the $\Delta S_w / \Delta \langle H_w \rangle \rightarrow 0$ limit. This is in accordance with the claims that $T_w \rightarrow \infty$ limit of an absorption refrigerator, is analogous to a power refrigerator [83]. The price for this choice of the initial state of the battery is that the number of batteries diverges as $\Delta S_w / \Delta \langle H_w \rangle \rightarrow 0$.

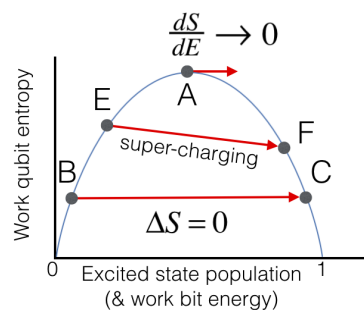


Figure 3. For infinitesimal changes (weak coupling), it is preferable to start with a battery qubit that is close to the fully mixed state (point A) where $dS/dE = 0$. For larger changes, it is preferable to generate a permutation that conserves the entropy and creates population inversion ($B \rightarrow C$ line). While $\Delta S = 0$ for the battery is analogous to classical field work repositories, in two-level batteries, it is possible to super-charge the batteries ($E \rightarrow F$) so that their energy is increased while their entropy is reduced (see also Figure 4).

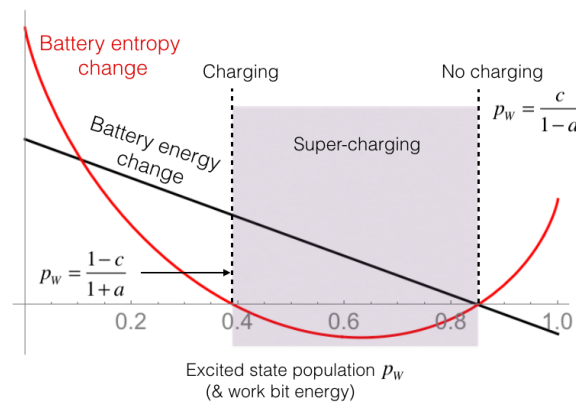


Figure 4. For a given engine, the changes in energy (**black**) and entropy (**red**) of the battery are plotted as a function of the initial excited state probability p_w of the battery. a, b and c are the population of levels 1–3 of the engine just before the interaction with the battery starts. The shaded area shows the super-charging regime where the battery is not only charged but also purified. This can only be done by strong interaction between the engine and the battery. The left border corresponds to regular charging where the energy is increased but the entropy of the battery remains the same.

In the semi-classical field approximation, the field generates a unitary operation that does not change the entropy of the system. This is often addressed as pure work as there is no entropy change in the system. However, when modeling the classical field explicitly, one finds that the source of the classical field actually gains some entropy. To counter this effect, the battery has to be prepared in a special state [30,67] or a feedback scheme must be applied [84]. Here, we suggest doing the exact opposite and applying an interaction that will generate a unitary transformation on the battery but will generate some entropy in the engine. Consider Point B in Figure 3, a full swap to Point C will increase the energy but will leave the entropy fixed. In general, this will *increase the entropy of the machine*. Let the initial state of the engine be $\rho_e = \text{diag}\{a, b, c\}$ and the initial state of the work qubit be $\rho_w = \text{diag}\{1 - p_w, p_w\}$. After a *full swap* interaction we get:

$$\begin{pmatrix} a & & \\ & b & \\ & & c \end{pmatrix}_e, \begin{pmatrix} 1 - p_w & \\ & p_w \end{pmatrix}_w \rightarrow \begin{pmatrix} a & & \\ & (1 - a)(1 - p_w) & \\ & & (1 - a)p_w \end{pmatrix}_e, \begin{pmatrix} b + a(1 - p_w) & 0 \\ 0 & c + ap_w \end{pmatrix}_w. \tag{8}$$

If $a = 0$, a regular full swap takes place between levels 2 and 3 of the engine and levels 1 and 2 of the battery. If $a = 1$, there is no population in level 2&3 so nothing happens and levels 1&2 of the battery remain unchanged. This rule follows from the condition that guarantees energy conservation $\rho'_e - \rho_e = -(\rho'_w - \rho_w)$. Any population change in one particle must be compensated by an opposite change in the other particle (the energy levels are equal in our model). Now, we demand that this transformation of the battery will generate a full swap, that is $\rho'_w = \text{diag}\{p_w, 1 - p_w\}$. This leads to the condition $c + ap_w = 1 - p_w$ or

$$p_w = \frac{1 - c}{1 + a}. \tag{9}$$

Note that p_w defines a temperature through the Gibbs factor: $p_w/(1 - p_w) = \exp(-E_w/T_w)$. After the full swap, the temperature of levels 2&3 of the engine, is now T_w . It is simple to show from the positivity of the quantum mutual information that the entropy of the engine has increased. This entropy increase is associated with the formation of correlation (for the full swap it is strictly classical). When the total population on the subspace of interest on both sides is not equal (e.g., $a \neq 0$ in the example above), classical correlation forms. If the engine is measured, the marginal distribution of the battery changes. Another way to see the presence of correlation is the following. The unitary conserves the total entropy. However, the entropy of the reduced state of the battery does not change while the reduced entropy of the engine does change. This implies that the mutual information is larger than zero. This classical correlation formation can be avoided by replacing the qubit batteries with qutrit batteries whose initial state is $\rho_w = \text{diag}\{a, c, b\}$ (note the flip of b and c). In this case, the full swap operation will not generate any correlation between the engine and the battery.

The full swap is a strong coupling operation. Here, strong coupling was used to make a more efficient battery charging mechanism compared to the $T_w \rightarrow \infty$ alternative in the weak coupling limit.

3.2.2. Beyond the Semi-Classical Limit of the Driving Field

When the work repository can be described by a classical field, no entropy accounting is carried out for the work repository. However, for an explicit battery the possible changes in the entropy of the battery have to be studied. In this subsection, it is shown that these changes can actually be useful. As illustrated in the $E \rightarrow F$ trajectory in Figure 3, it is possible to increase the energy while reducing the entropy. We name this process “super-charging”. In a *regular* charging, the energy increases but the entropy of the battery remains fixed. This corresponds to executing a unitary operation on the battery. In *sub-charging*, the energy is increased but so is the entropy. Heat flow to a thermal bath in the weak system-bath coupling limit is an example of sub-charging. Strictly speaking, in super-charging, the machine does not exactly correspond to an engine, since the energy change in the battery is associated with an entropy change as well. Nevertheless, this change in entropy is a welcomed one, as entropy reduction is hard to achieve and often requires some additional resources. In Figure 4, we show an explicit example for an initial engine state with populations $\{a, b, c\} = \{0.056, 0.074, 0.4\}$ as a function of the initial excited state population of the battery p_w . The shaded area corresponds to super-charging. The left boundary of the shaded regime corresponds to regular charging and is given by the $dS = 0$ condition Equation (9). The right boundary is given by the condition $\Delta E = 0$. Using Equation (8) $\Delta E = 0$ leads to the right boundary condition $p_w = c/1 - a = c/(b + c)$. This condition means that population ratio in the engine qutrit and in the battery is the same. Hence, nothing happens when the swap is carried out. This zero change in population also leads to $\Delta S = 0$ at this point.

3.3. Higher Order Splittings

The regime of equivalence studied in Section 3.1 and in [1] is determined by the use of the Strang decomposition for the evolution operator. Although higher order decompositions do exist, they involve coefficients with alternating signs [85]. In the Markovian case, this is not physical since a bath that generates evolution of the form $\exp(-\mathcal{L}t)$ is not physical (where $\exp(+\mathcal{L}t)$ is the standard Lindblad evolution). In the present paper, instead of non unitary evolution of the reduced state of the engine, we consider the global evolution operator of all the components. The global evolution is unitary and its generators, the interaction Hamiltonian, are all Hermitian. Hence, there is no problem to have for example $\exp(+iH_{ec}t)$ instead of $\exp(-iH_{ec}t)$. It simply means an interaction term with opposite sign. This facilitates the use of higher order decompositions in order to make machines with more strokes and a larger regime of equivalence.

In [86], Yoshida introduced a very elegant method to construct higher order decompositions. Let $U_{s^2}(t) = U^{\text{simul}}(t) + O[(\frac{s}{\hbar})^4]$ stand for an evolution operator that has a correction of order s^3 with

respect to $U^{simul}(t)$. It can be, for example, a four-stroke or two-stroke engine. As shown in [86], a fourth order evolution operator $U_{s^4}(t)$ can be constructed from $U_{s^2}(t)$ in the following way:

$$\begin{aligned} U_{s^4}(t) &= U_{s^4}(x_1 t) U_{s^4}(x_0 t) U_{s^4}(x_1 t), \\ \{x_0, x_1\} &= \left\{ \frac{-2^{1/3}}{1-2^{1/3}}, \frac{1}{1-2^{1/3}} \right\}, \end{aligned} \quad (10)$$

where $U_{s^4}(t) = U^{simul}(t) + O[(\frac{s}{\hbar})^5]$. By applying the same arguments as before, when the cycle starts with fresh uncorrelated bath and battery particles, the correction to the work and heat are $O[(\frac{s}{\hbar})^6]$. The Yoshida method is powerful since it can be repeated, with different x_0, x_1 coefficients, to gain operators that are even closer to the simultaneous machine. Physically, Equation (10) can be interpreted as a regular $U_{s^2}(t)$ machine where the stroke durations alternate every cycle. Figure 2b shows the ratio of the power of various engines with respect to the simultaneous engine. While in the Strang four-stroke and two-stroke machine, the *power* deviation from the simultaneous machine is second order in the action, the power of the Yoshida engine of order four deviates from the simultaneous machine only in the fourth order in the action.

Two-stroke and four-stroke engines naturally emerge from practical considerations. Two-stroke engines emerge when it is easier to thermalize simultaneously the hot and cold manifolds. Four-stroke engines emerge when it is easier to thermalize one manifold at a time. In contrast, the Yoshida decomposition Equation (10) does not split the simultaneous engine into more basic or simpler operations compared to the two-stroke and four-stroke machines. Thus, the practical motivation for actually constructing Yoshida-like higher order machines is not obvious at all at this point. Nevertheless, our main point in this context is that higher order machines are forbidden in Markovian dynamics and are allowed in the non-Markovian machines studied here.

4. Conclusions

It has been demonstrated that the principle of thermodynamic equivalence of heat machine types is valid beyond Markovianity. We find higher order equivalence relations that do not exist in the Markovian regime. In addition, it was shown that the strong coupling limit enables delivery of finite work to the battery without increasing its entropy. It also enables charging and reducing the entropy of the battery at the same time. In our setup, we introduced heat exchangers to mediate between the machine and the baths. Heat exchangers significantly simplify the analysis, but they also have a significant practical value. They remove the strong dependence on the finer properties of the baths and allow more flexible machine operating regimes while still using a simple Markovian bath.

Acknowledgments: This work was supported by the Israeli science foundation. Part of this work was supported by the COST Action MP1209 “Thermodynamics in the quantum regime”. Raam Uzdin cordially thanks the support of the Kenneth Lindsay trust fund.

Author Contributions: All authors contributed equally. All authors have read and approved the final manuscript.

Conflicts of Interest: The authors declare no conflict of interest.

References

1. Uzdin, R.; Levy, A.; Kosloff, R. Equivalence of Quantum Heat Machines, and Quantum-Thermodynamic Signatures. *Phys. Rev. X* **2015**, *5*, 031044.
2. Mitchison, M.T.; Woods, M.P.; Prior, J.; Huber, M. Coherence-assisted single-shot cooling by quantum absorption refrigerators. *New J. Phys.* **2015**, *17*, 115013, doi:10.1088/1367-2630/17/11/115013.
3. Goold, J.; Huber, M.; Riera, A.; del Rio, L.; Skrzypczyk, P. The role of quantum information in thermodynamics—A topical review. *J. Phys. A Math. Theor.* **2016**, *49*, 143001.
4. Vinjanampathy, S.; Anders, J. Quantum Thermodynamics. **2013**, doi:10.3390/e15062100.
5. Millen, J.; Xuereb, A. Perspective on quantum thermodynamics. *New J. Phys.* **2016**, *18*, 011002.
6. Scovil, H.E.D.; Schulz-DuBois, E.O. Three-Level Masers as Heat Engines. *Phys. Rev. Lett.* **1959**, *2*, 262–263.

7. Geva, E.; Kosloff, R. The Three-Level Quantum Amplifier as a Heat Engine: A Study in Finite-Time Thermodynamics. *Phys. Rev. E* **1994**, *49*, 3903–3918.
8. Geva, E.; Kosloff, R. The Quantum Heat Engine and Heat Pump: An Irreversible Thermodynamic Analysis of the Three-Level Amplifier. *J. Chem. Phys.* **1996**, *104*, 7681–7698.
9. Alicki, R. The quantum open system as a model of the heat engine. *J. Phys A Math. Gen.* **1979**, *12*, L103, doi:10.1088/0305-4470/12/5/007.
10. Kosloff, R. A Quantum Mechanical Open System as a Model of a Heat Engine. *J. Chem. Phys.* **1984**, *80*, 1625–1631.
11. Feldmann, T.; Kosloff, R. Performance of Discrete Heat Engines and Heat Pumps in Finite Time. *Phys. Rev. E* **2000**, *61*, 4774–4790.
12. Rezek, Y.; Kosloff, R. Irreversible performance of a quantum harmonic heat engine. *New J. Phys.* **2006**, *8*, 83, doi:10.1088/1367-2630/8/5/083.
13. Kosloff, R.; Levy, A. Quantum Heat Engines and Refrigerators: Continuous Devices. *Annu. Rev. Phys. Chem.* **2014**, *65*, 365–393.
14. Harbola, U.; Rahav, S.; Mukamel, S. Quantum heat engines: A thermodynamic analysis of power and efficiency. *Euro. Phys. Lett.* **2012**, *99*, 50005, doi:10.1209/0295-5075/99/50005.
15. Allahverdyan, A.E.; Hovhannisyanyan, K.; Mahler, G. Optimal refrigerator. *Phys. Rev. E* **2010**, *81*, 051129.
16. Linden, N.; Popescu, S.; Skrzypczyk, P. How Small Can Thermal Machines Be? The Smallest Possible Refrigerator. *Phys. Rev. Lett.* **2010**, *105*, 130401.
17. Henrich, M.J.; Rempp, F.; Mahler, G. Quantum thermodynamic Otto machines: A spin-system approach. *Eur. Phys. J.* **2005**, *151*, 157–165.
18. Skrzypczyk, P.; Short, A.J.; Popescu, S. Work extraction and thermodynamics for individual quantum systems. *Nat. Commun.* **2014**, *5*, 4185, doi:10.1038/ncomms5185.
19. Gelbwaser-Klimovsky, D.; Alicki, R.; Kurizki, G. Work and energy gain of heat-pumped quantized amplifiers. *Europhys. Lett.* **2013**, *103*, 60005, doi:10.1209/0295-5075/103/60005.
20. Kolář, M.; Gelbwaser-Klimovsky, D.; Alicki, R.; Kurizki, G. Quantum Bath Refrigeration towards Absolute Zero: Challenging the Unattainability Principle. *Phys. Rev. Lett.* **2012**, *109*, 090601.
21. Alicki, R. Quantum Thermodynamics: An Example of Two-Level Quantum Machine. *Open Syst. Inf. Dyn.* **2014**, *21*, 1440002, doi:10.1142/S1230161214400022.
22. Quan, H.; Liu, Y.X.; Sun, C.; Nori, F. Quantum thermodynamic cycles and quantum heat engines. *Phys. Rev. E* **2007**, *76*, 031105.
23. Roßnagel, J.; Abah, O.; Schmidt-Kaler, F.; Singer, K.; Lutz, E. Nanoscale Heat Engine Beyond the Carnot Limit. *Phys. Rev. Lett.* **2014**, *112*, 030602.
24. Binder, F.; Vinjanampathy, S.; Modi, K.; Goold, J. Quantum thermodynamics of general quantum processes. *Phys. Rev. E* **2015**, *91*, 032119.
25. Correa, L.A.; Palao, J.P.; Alonso, D.; Adesso, G. Quantum-enhanced absorption refrigerators. *Sci. Rep.* **2014**, *4*, 3949, doi:10.1038/srep03949.
26. Dorner, R.; Clark, S.; Heaney, L.; Fazio, R.; Goold, J.; Vedral, V. Extracting quantum work statistics and fluctuation theorems by single-qubit interferometry. *Phys. Rev. Lett.* **2013**, *110*, 230601.
27. Correa, L.A.; Palao, J.P.; Adesso, G.; Alonso, D. Performance bound for quantum absorption refrigerators. *Phys. Rev. E* **2013**, *87*, 042131.
28. Dorner, R.; Goold, J.; Cormick, C.; Paternostro, M.; Vedral, V. Emergent thermodynamics in a quenched quantum many-body system. *Phys. Rev. Lett.* **2012**, *109*, 160601.
29. Del Campo, A.; Goold, J.; Paternostro, M. More bang for your buck: Super-adiabatic quantum engines. *Sci. Rep.* **2014**, *4*, 6208, doi:10.1038/srep06208.
30. Malabarba, A.S.; Short, A.J.; Kammerlander, P. Clock-Driven Quantum Thermal Engines. *New J. Phys.* **2015**, *17*, 045027.
31. Gelbwaser-Klimovsky, D.; Niedenzu, W.; Kurizki, G. Chapter Twelve—Thermodynamics of Quantum Systems Under Dynamical Control. In *Advances In Atomic, Molecular, and Optical Physics*; Academic Press: Salt Lake City, UT, USA, 2015; Volume 64, pp. 329–407.
32. Whitney, R.S. Most efficient quantum thermoelectric at finite power output. *Phys. Rev. Lett.* **2014**, *112*, 130601.
33. Allahverdyan, A.E.; Hovhannisyanyan, K.; Mahler, G. Optimal refrigerator. *Phys. Rev. E* **2010**, *81*, 051129.

34. Mari, A.; Eisert, J. Cooling by Heating: Very Hot Thermal Light Can Significantly Cool Quantum Systems. *Phys. Rev. Lett.* **2012**, *108*, 120602.
35. Bakr, W.S.; Preiss, P.M.; Tai, M.E.; Ma, R.; Simon, J.; Greiner, M. Orbital excitation blockade and algorithmic cooling in quantum gases. *Nature* **2011**, *480*, 500–503.
36. Baugh, J.; Moussa, O.; Ryan, C.A.; Nayak, A.; Laflamme, R. Experimental implementation of heat-bath algorithmic cooling using solid-state nuclear magnetic resonance. *Nature* **2005**, *438*, 470–473.
37. Boykin, P.O.; Mor, T.; Roychowdhury, V.; Vatan, F.; Vrijen, R. Algorithmic cooling and scalable NMR quantum computers. *Proc. Natl. Acad. Sci. USA* **2002**, *99*, 3388–3393.
38. Rempp, F.; Michel, M.; Mahler, G. Cyclic Cooling Algorithm. *Phys. Rev. A* **2007**, *76*, 032325.
39. Segal, D.; Nitzan, A. Molecular heat pump. *Phys. Rev. E* **2006**, *73*, 026109.
40. Schulman, L.J.; Mor, T.; Weinstein, Y. Physical limits of heat-bath algorithmic cooling. *Phys. Rev. Lett.* **2005**, *94*, 120501.
41. Oscar Boykin, P.; Mor, T.; Roychowdhury, V.; Vatan, F.; Vrijen, R. Algorithmic cooling and scalable NMR quantum computer. *Proc. Nat. Acad. Sci.* **2002**, *99*, 3388–3393.
42. Skrzypczyk, P.; Brunner, N.; Linden, N.; Popescu, S. The smallest refrigerators can reach maximal efficiency. *J. Phys. A Math. Theor.* **2011**, *44*, 492002.
43. Brandner, K.; Bauer, M.; Schmid, M.T.; Seifert, U. Coherence-enhanced efficiency of feedback-driven quantum engines. *New J. Phys.* **2015**, *17*, 065006.
44. Bulnes Cuetara, G.; Engels, A.; Esposito, M. Stochastic thermodynamics of rapidly driven quantum systems. *New J. Phys.* **2015**, *17*, 055002.
45. Perarnau-Llobet, M.; Hovhannisyan, K.V.; Huber, M.; Skrzypczyk, P.; Brunner, N.; Acín, A. Extractable Work from Correlations. *Phys. Rev. X* **2015**, *5*, 041011.
46. Roßnagel, J.; Dawkins, S.T.; Tolazzi, K.N.; Abah, O.; Lutz, E.; Schmidt-Kaler, F.; Singer, K. A single-atom heat engine. Available online: <http://arxiv.org/abs/1510.03681> (accessed on 23 March 2016).
47. Venturelli, D.; Fazio, R.; Giovannetti, V. Minimal self-contained quantum refrigeration machine based on four quantum dots. *Phys. Rev. Lett.* **2013**, *110*, 256801.
48. Bergenfeldt, C.; Samuelsson, P.; Sothmann, B.; Flindt, C.; Büttiker, M. Hybrid microwave-cavity heat engine. *Phys. Rev. Lett.* **2014**, *112*, 076803.
49. Niskanen, A.; Nakamura, Y.; Pekola, J. Information entropic superconducting microcooler. *Phys. Rev. B* **2007**, *76*, 174523.
50. Brask, J.B.; Haack, G.; Brunner, N.; Huber, M. Autonomous quantum thermal machine for generating steady-state entanglement. *New J. Phys.* **2015**, *17*, 113029.
51. Campisi, M.; Pekola, J.; Fazio, R. Nonequilibrium fluctuations in quantum heat engines: Theory, example, and possible solid state experiments. *New J. Phys.* **2015**, *17*, 035012.
52. Pekola, J.P. Towards quantum thermodynamics in electronic circuits. *Nat. Phys.* **2015**, *11*, 118–123.
53. Fialko, O.; Hallwood, D. Isolated quantum heat engine. *Phys. Rev. Lett.* **2012**, *108*, 085303.
54. Zhang, K.; Bariani, F.; Meystre, P. Quantum optomechanical heat engine. *Phys. Rev. Lett.* **2014**, *112*, 150602.
55. Dechant, A.; Kiesel, N.; Lutz, E. All-Optical Nanomechanical Heat Engine. *Phys. Rev. Lett.* **2015**, *114*, 183602.
56. Thierschmann, H.; Sánchez, R.; Sothmann, B.; Arnold, F.; Heyn, C.; Hansen, W.; Buhmann, H.; Molenkamp, L.W. Three-terminal energy harvester with coupled quantum dots. *Nat. Nanotechnol.* **2015**, *10*, 854–858.
57. Sánchez, R.; Büttiker, M. Optimal energy quanta to current conversion. *Phys. Rev. B* **2011**, *83*, 085428.
58. Roche, B.; Roulleau, P.; Jullien, T.; Jompol, Y.; Farrer, I.; Ritchie, D.; Glatli, D. Harvesting dissipated energy with a mesoscopic ratchet. *Nat. Commun.* **2015**, *6*, 6383, doi:10.1038/ncomms7738.
59. Hartmann, F.; Pfeiffer, P.; Höfling, S.; Kamp, M.; Worschech, L. Voltage fluctuation to current converter with coulomb-coupled quantum dots. *Phys. Rev. Lett.* **2015**, *114*, 146805.
60. Sothmann, B.; Sánchez, R.; Jordan, A.N.; Büttiker, M. Rectification of thermal fluctuations in a chaotic cavity heat engine. *Phys. Rev. B* **2012**, *85*, 205301.
61. Sagawa, T. Second law-like inequalities with quantum relative entropy: An introduction. *Lect. Quantum Comput. Thermodyn. Stat. Phys.* **2012**, *8*, 127. Available online: <http://arxiv.org/abs/1202.0983> (accessed on 2 April 2016).
62. Kammerlander, P.; Anders, J. Quantum measurement and its role in thermodynamics. Available online: <http://arxiv.org/abs/1502.02673> (accessed on 29 March 2016).

63. Jaramillo, J.; Beau, M.; del Campo, A. Quantum Supremacy of Many-Particle Thermal Machines. Available online: <http://arxiv.org/abs/1510.04633> (accessed on 3 April 2016).
64. Lostaglio, M.; Jennings, D.; Rudolph, T. Description of quantum coherence in thermodynamic processes requires constraints beyond free energy. *Nat. Commun.* **2015**, *6*, 6383, doi:10.1038/ncomms7383.
65. Ćwikliński, P.; Studziński, M.; Horodecki, M.; Oppenheim, J. Limitations on the Evolution of Quantum Coherences: Towards Fully Quantum Second Laws of Thermodynamics. *Phys. Rev. Lett.* **2015**, *115*, 210403.
66. Korzekwa, K.; Lostaglio, M.; Oppenheim, J.; Jennings, D. The extraction of work from quantum coherence. Available online: <http://arxiv.org/abs/1506.07875> (accessed on 22 February 2016).
67. Åberg, J. Catalytic coherence. *Phys. Rev. Lett.* **2014**, *113*, 150402.
68. Levy, A.; Kosloff, R. Quantum absorption refrigerator. *Phys. Rev. Lett.* **2012**, *108*, 070604.
69. Breuer, H.-P.; Petruccione, F. *Open Quantum Systems*; Oxford University Press: New York, NY, USA, 2002.
70. Gallego, R.; Riera, A.; Eisert, J. Thermal machines beyond the weak coupling regime. *New J. Phys.* **2014**, *16*, 125009, doi:10.1088/1367-2630/16/12/125009.
71. Esposito, M.; Ochoa, M.A.; Galperin, M. Quantum Thermodynamics: A Nonequilibrium Green's Function Approach. *Phys. Rev. Lett.* **2015**, *114*, 080602.
72. Gelbwaser-Klimovsky, D.; Aspuru-Guzik, A. Strongly coupled quantum heat machines. *J. Phys. Chem. Lett.* **2015**, *6*, 3477–3482.
73. Uzdin, R.; Kosloff, R. The multilevel four-stroke swap engine and its environment. *New J. Phys.* **2014**, *16*, 095003.
74. Rybár, T.; Filippov, S.N.; Ziman, M.; Bužek, V. Simulation of indivisible qubit channels in collision models. *J. Phys. B At. Mol. Opt. Phys.* **2012**, *45*, 154006.
75. Ziman, M.; Štelmachovič, P.; Bužek, V. Description of quantum dynamics of open systems based on collision-like models. *Open Syst. Inf. Dyn.* **2005**, *12*, 81–91.
76. Gennaro, G.; Benenti, G.; Palma, G.M. Relaxation due to random collisions with a many-qudit environment. *Phys. Rev. A* **2009**, *79*, 022105.
77. Gennaro, G.; Benenti, G.; Palma, G.M. Entanglement dynamics and relaxation in a few-qubit system interacting with random collisions. *Europhys. Lett.* **2008**, *82*, 20006, doi:10.1209/0295-5075/82/20006.
78. Woods, M.P.; Ng, N.; Wehner, S. The maximum efficiency of nano heat engines depends on more than temperature. Available online: <http://arxiv.org/abs/1506.02322> (accessed on 1 April 2016).
79. Uzdin, R. Coherence recycling, collective operation, and coherence induced reversibility in quantum heat engines. Available online: <http://arxiv.org/abs/1509.06289> (accessed on 1 April 2016).
80. De Raedt, H. Product formula algorithms for solving the time dependent Schrödinger equation. *Comput. Phys. Rep.* **1987**, *7*, 1–72, doi:10.1016/0167-7977(87)90002-5.
81. Feit, M.; Fleck, J.; Steiger, A. Solution of the Schrödinger equation by a spectral method. *J. Comput. Phys.* **1982**, *47*, 412–433.
82. Jahnke, T.; Lubich, C. Error bounds for exponential operator splittings. *BIT Numer. Math.* **2000**, *40*, 735–744.
83. Levy, A.; Alicki, R.; Kosloff, R. Quantum refrigerators and the third law of thermodynamics. *Phys. Rev. E* **2012**, *85*, 061126.
84. Levy, A.; Diósi, L.; Kosloff, R. Quantum Flywheel. Available online: <http://arxiv.org/abs/1602.04322> (accessed on 21 March 2016).
85. Blanes, S.; Casas, F. On the necessity of negative coefficients for operator splitting schemes of order higher than two. *Appl. Numer. Math.* **2005**, *54*, 23–37.
86. Yoshida, H. Construction of higher order symplectic integrators. *Phys. Lett. A* **1990**, *150*, 262–268.

